Journal of Computer Assisted Tomography

Evaluation of Lung Radiofrequency Ablation with Dual-energy Computed Tomography: Analysis of Tumor Composition and Lung Perfusion

--Manuscript Draft--

Manuscript Number:	
Full Title:	Evaluation of Lung Radiofrequency Ablation with Dual-energy Computed Tomography: Analysis of Tumor Composition and Lung Perfusion
Article Type:	Original Article
Keywords:	composition analysis; dual-energy computed tomography; lung perfusion; lung radiofrequency ablation
Corresponding Author:	Takao Hiraki Okayama, JAPAN
Corresponding Author Secondary Information:	
Corresponding Author's Institution:	
Corresponding Author's Secondary Institution:	
First Author:	Koji Tomita
First Author Secondary Information:	
Order of Authors:	Koji Tomita
	Takao Hiraki
	Hideo Gobara
	Hiroyasu Fujiwara
	Toshihiro Iguchi
	Yusuke Matsui
	Susumu Kanazawa
Order of Authors Secondary Information:	
Manuscript Region of Origin:	JAPAN
Abstract:	Objective: To evaluate radiofrequency ablation (RFA) of lung tumors with dual-energy computed tomography (DECT) while focusing on tumor composition and lung perfusion. Methods: The 36 tumors in 25 patients were included. DECT was performed before RFA and at 2 days, 1, 3, and 6 months thereafter. The effective atomic number (Zeff) of the tumors before RFA was compared with the Zeff at each follow-up using the paired t test. Lung perfusion was evaluated by iodine map images. When decreased perfusion was suspected after RFA, lung perfusion scintigraphy was performed. Results: The mean Zeff of the tumors significantly ($P < 0.001$) decreased at each follow up, compared with that before RFA. Lung perfusion in the parenchyma peripheral to the tumors appeared to decrease at 2 days in 9 tumors, which was confirmed by scintigraphy in 7 tumors. Conclusions: DECT was useful by providing additional information on tumor composition and lung perfusion.

Abstract

Objective: To evaluate radiofrequency ablation (RFA) of lung tumors with dual-energy computed tomography (DECT) while focusing on tumor composition and lung perfusion.

Methods: The 36 tumors in 25 patients were included. DECT was performed before RFA and at 2 days, 1, 3, and 6 months thereafter. The effective atomic number (Z_{eff}) of the tumors before RFA was compared with the Z_{eff} at each follow-up using the paired *t* test. Lung perfusion was evaluated by iodine map images. When decreased perfusion was suspected after RFA, lung perfusion scintigraphy was performed.

Results: The mean Z_{eff} of the tumors significantly ($P < 0.001$) decreased at each follow up, compared with that before RFA. Lung perfusion in the parenchyma peripheral to the tumors appeared to decrease at 2 days in 9 tumors, which was confirmed by scintigraphy in 7 tumors.

Conclusions: DECT was useful by providing additional information on tumor composition and lung perfusion.

Key words: composition analysis, dual-energy computed tomography, lung perfusion, lung radiofrequency ablation

Introduction

Dual-energy computed tomography (DECT) enables scanning simultaneously at low- and high-energy levels, typically 80 kVp and 140 kVp, respectively. Different attenuation coefficients obtained by the 2 energy levels are helpful in discriminating between different material compositions. For example, Wisenbaugh et al. [1] examined the composition of renal stones with DECT and found that they could differentiate non-uric acid stones from uric acid stones with an accuracy of 93% (14/15). Li et al. [2] showed that the effective atomic number (Z_{eff}) was significantly higher for benign thyroid nodules than for thyroid papillary carcinomas, which indicates the potential to differentiate between benign and malignant thyroid nodules. In addition to composition analysis, DECT may allow visualization of parenchymal iodine distribution (the iodine map) as a representation of lung perfusion. An iodine map is useful for diagnosing pulmonary embolism; its sensitivity and specificity for detecting perfusion defects due to pulmonary embolism was 96% and 76%, respectively, in a study by Nakazawa et al. [3] and 100% and 100%, respectively, in a study by Thieme et al. [4].

Since its first clinical application was reported in 2000 [5], radiofrequency ablation (RFA) has been used to treat lung cancer [6, 7]. However, local progression after RFA is not rare, occurring in 10% or more of patients [6, 7]. Local progression is

usually diagnosed by comparing the size and geometry of the ablation zone on serial follow-up CT images. Local tumor progression is diagnosed when the ablation zone is enlarged or when an irregular, scattered, nodular, or eccentric focus appears in the ablation zone. We hypothesized that the composition of lung tumors was altered after RFA and that analyzing tumor composition before the size and geometry of the ablation zone changed could be helpful for diagnosing local progression. We furthermore presumed that the influence of RFA on perfusion of the parenchyma peripheral to the treated tumor might be evaluated by lung perfusion analysis. However, the alteration in tumor composition and perfusion by lung RFA is poorly understood. The purpose of this study was therefore to prospectively evaluate RFA of lung tumors with DECT while focusing on tumor composition and lung perfusion.

Materials and Methods

Study population

This study was prospectively designed and performed from August 2012 through May 2013. Approval from the institutional review board (approval number 1468) and informed consent from the patients were obtained. During the 10-months study period, 50 lung tumors in 31 patients were treated with RFA. Among those, 14

tumors in 6 patients were excluded from the analysis of tumor composition or lung perfusion. The reasons for exclusion were: (1) the patient was lost to follow-up; (2) the tumor was too small (4mm) to allow placement of the ROI for tumor composition analysis avoiding partial volume effect; (3) the lesion was a pure ground-glass opacity (the Z_{eff} value of the lesion was affected by alveolar air within the lesion); (4) because the tumor was close to the ablation zone by previous RFA, the ROI for tumor composition analysis overlapped the previous ablation zone; (5) the tumor sloughed off completely after RFA and the ablation zone became cavitary, interfering with analysis; and (6) artifact from coils used to embolize a pulmonary artery pseudoaneurysm after RFA interfered with the analyses of both tumor composition and pulmonary perfusion. Therefore, analyses of tumor composition and lung perfusion were performed for the remaining 36 tumors in 25 patients. Table 1 summarizes the population included in the analysis. All 36 tumors were metastatic lung cancer from various types of primary cancer. The diagnosis of metastatic lung cancer was pathologically proven with biopsy in 3 tumors. In the other 33 tumors, the diagnosis was made based on the results of serial follow-up CT images without pathological proof, i.e., new lung nodules were diagnosed as metastatic lung cancer. Four tumors were accompanied with elevation of specific tumor marker. Eighteen tumors developed in patients with a history of resection

of lung metastasis.

RFA techniques

The detail of RFA techniques in our institution is described elsewhere in the medical literature [8]. In brief, all procedures were percutaneously performed under CT-fluoroscopic guidance in an inpatient setting. A multitined expandable electrode (LeVeen; Boston Scientific, Natick, MA, USA) was used for 35 tumors and an internally cooled electrode (Cool-tip; Covidien, Mansfield, MA, USA) was used for 1 tumor. After administering the anesthetic, the electrode was introduced into the tumor and connected to a generator. A given radiofrequency energy was applied in accordance with our ablation protocol [8]. The procedure aimed to ablate the tumor plus at least a 5-mm margin.

CT examinations

Chest CT was performed with a DECT scanner (Discovery CT750HD; GE Healthcare, Milwaukee, WI, USA) in dual-energy mode within 8 weeks before RFA and at 2 days, 1 month, 3 months, and 6 months after RFA based on our follow up protocol. After the patients underwent plain CT scanning, a contrast-enhanced CT scan was

performed at 30 s and 90 s after the intravenous administration of 100 mL of a contrast medium (iopamidol, 300 mgI/mL [Iopamiron 300]; Bayer, Osaka, Japan) at a rate of 3 mL/s. Data were obtained with the following parameters: spectral imaging scan mode with fast tube voltage switching between 80 kVp and 140 kVp; tube current, 630 mA; helical pitch, 0.984:1; rotation time, 0.5 s; and collimation thickness, 0.625 mm × 64. Axial and coronal images were reconstructed at 5-mm thickness and 5-mm intervals. Axial images were also reconstructed at 1.25-mm thickness and 1.25-mm intervals.

Analysis of tumor composition

The tumor composition was analyzed using plain axial images with 1.25-mm thickness before RFA and at 2 days, 1 month, 3 months, and 6 months after RFA using the Gemstone Spectral Imaging (GSI) viewer (GE Healthcare). The quantitative parameter that was evaluated was the Z_{eff} of the tumors, which was estimated by placing the region of interest (ROI) onto the target. A radiologist (K.T.) with 9-year experience of lung RFA placed the ROI. A case of ROI placement is shown in Figure 1. On CT images before RFA, the ROI was placed on the tumors at the level where the tumors had the largest cross-sectional area. The ROI was created as large as possible inside the tumors avoiding surrounding lung parenchyma (Figure 1A). Two days to one month

after RFA, the tumor was identified on the CT images, although it was surrounded by ground-glass opacity, which indicated the ablated marginal parenchyma [9]. Thus, the ROI was placed on the tumor in a similar fashion as before RFA (Figure 1B, C). One to three months or more after RFA, the tumor and the ablated marginal parenchyma appeared on the CT images as a consolidated mass (the ablation zone) [9]. Therefore, the tumor itself could not be distinguished from surrounding marginal parenchyma. Then, the ROI was placed at the center of the ablation zone (Figure 1D, E). When the tumor or the ablation zone was cavitary, the ROI was positioned to avoid the cavity.

Analysis of lung perfusion

Although two phases of CT images were obtained after contrast administration, the images 30 s after contrast administration were used for evaluation of lung perfusion because iodine distribution of lung parenchyma (the iodine map) was clearer than the images 90 s after contrast administration. Lung perfusion was evaluated on axial and coronal CT images at 5-mm thickness before RFA and at 2 days, 1 month, 3 months, and 6 months after RFA using the GSI viewer (GE Healthcare), with which the iodine map was available. The iodine map images were visually evaluated with respect to perfusion of lung parenchyma peripheral to the ablated tumor. Evaluation was

performed by comparing the images at each post-RFA follow-up examination with the images before RFA; evaluation was made by the consensus of 2 radiologists with 20-year (T.H.) and 9-year experiences (K.T.) of lung RFA. If perfusion of lung parenchyma peripheral to the tumor appeared to decrease after RFA, lung perfusion scintigraphy and single-photon emission computed tomography combined with CT (SPECT/CT) were immediately performed for confirmation. A scintigram was obtained after the intravenous administration of 185 MBq of technetium-99m macroaggregated albumin. Immediately after the planar perfusion examination, SPECT/CT images were obtained using an integrated SPECT/CT system (Discovery NM/CT 670; GE Healthcare). The acquisition parameter for SPECT was a 128 × 128 matrix with 60 frames (15 s per frame). The scan parameters for SPECT/CT were 120 kV at 40 mAs and 200 mAs, 5-mm thickness and 5-mm interval, reconstructed at 1.25-mm thickness and 0.8-mm intervals. The images were fused with a dedicated workstation (Xeleris 3; GE Healthcare).

In the case of decreased parenchymal perfusion, the corresponding pulmonary arterial branches in the area of decreased perfusion were noted on CT images 30 s after contrast administration.

Statistical analysis

Data were missing for the analysis of tumor composition at 2 days and at 1 month after RFA in 4 tumors and 2 tumors, respectively. These missing data were simply excluded from the analysis of tumor composition. The Z_{eff} of the tumors before RFA was compared with the Z_{eff} at 2 days, 1 month, 3 months, and 6 months after RFA using the paired *t* test. A $P < 0.05$ indicated a statistically significant difference. The analysis was performed using commercially available software (SPSS software version 22.0; IBM, Chicago, IL, USA).

Results

Tumor composition

Compared to the Z_{eff} of the lung tumors before RFA, the Z_{eff} decreased in 91% (29/32) of tumors at 2 days, 97% (33/34) of tumors at 1 month, 97% (35/36) of tumors at 3 months, and 86% (31/36) of tumors at 6 months. The mean ± standard deviation (95% confidence interval [CI]) Z_{eff} of lung tumor was 8.27 ± 0.41 (8.12–8.41) before RFA, 7.97 ± 0.26 (7.88–8.06) at 2 days, 7.80 ± 0.21 (7.72–7.87) at 1 month, 7.74 ± 0.25 (7.66–7.83) at 3 months, and 7.88 ± 0.28 (7.78–7.97) at 6 months (Figure 2). Statistical significance existed between the Z_{eff} value before RFA and the Z_{eff} value at 2 days and

at 1 month, 3 months, and 6 months after RFA ($P < 0.001$ for each comparison) (Figure 2). None of the 36 tumors showed local progression in the 6 months after RFA.

Lung perfusion

Perfusion of the parenchyma peripheral to the tumors decreased 2 days after RFA in 9 (25%) tumors, based on lung perfusion analysis (Figures. 3 and 4). Decreased perfusion was confirmed by SPECT/CT images of lung perfusion scintigraphy in 7 of the 9 tumors (Figures 3 and 4). There was no decrease in the remaining 2 tumors. In all 7 cases of decreased perfusion that were confirmed by scintigraphy, the pulmonary arterial branches in the area of decreased perfusion were highly stenotic or occluded on CT images 2 days after RFA (Figure 4). At 1 month, 3 months, and 6 months after RFA, the area of decreased perfusion remained in 1 case but was not present in the remaining 6 cases. In all 7 cases of decreased perfusion that were confirmed by scintigraphy, the pulmonary arterial branches in the area of decreased perfusion remained severely damaged or occluded at 1 month, 3 months, and 6 months after RFA.

Discussion

Previous studies have described the use of DECT to evaluate the outcomes of

RFA. Lee et al. [10] reported that DECT scanning with virtual noncontrast images was useful for reducing radiation dosage while maintaining acceptable image quality in the assessment of RFA of hepatocellular carcinoma. Park et al. [11] also demonstrated the usefulness of virtual noncontrast images for evaluating RFA of renal cell carcinoma. To our knowledge, however, there have been no studies of the use of dual-energy CT for composition and perfusion analysis of RFA of lung tumors.

The Z_{eff} is a quantitative index to characterize the composition of tissue [2]. The Z_{eff} is determined by applying the ratio of the linear attenuation coefficients at 2 energies to the curve of known elements of known atomic numbers [12]. In this study, the Z_{eff} of the tumors significantly decreased at each follow-up point after RFA without any overlap between the 95% CIs of the Z_{eff} of the tumors before and after RFA. Although the exact mechanism of the decrease in Z_{eff} after RFA cannot be determined, we assumed that necrosis of tumors was related to the decrease of Z_{eff} after RFA. This result suggests the possibility of detecting local tumor progression by measuring the Z_{eff} of tumors, i.e., If Z_{eff} of the tumors decreases after RFA but subsequently elevates during follow-up, it might indicate local tumor progression.

Histopathology in a previous animal study showed that small pulmonary arteries could be occluded by thrombus formation after lung RFA [13]. However, the

influence of RFA on lung parenchymal perfusion in clinical cases is poorly understood. This study showed that lung perfusion occasionally decreased in the parenchyma peripheral to the treated tumor at 2 days. It seems of value to recognize that lung perfusion may be damaged in the region wider than the ablated parenchyma, especially in case of RFA for the patient with severely limited pulmonary function. The corresponding pulmonary arterial branches were highly stenotic or occluded in the area of decreased perfusion. However, perfusion recovered in most cases. Mechanisms for such recovery may include recanalization of the thrombosed artery, collateral development between pulmonary arteries, and supply by bronchial arteries. Considering that pulmonary arterial branches remained highly stenotic or occluded after perfusion recovered, one or both of the latter two mechanisms may be at work.

This study has several limitations. The study comprised a relatively small population with a short follow-up period. Tumor composition analysis included various types of lung tumors. Most lung metastases were not pathologically proven. Because the tumor itself could not be distinguished from ablated marginal parenchyma on CT images 1 month or later after RFA, it was difficult to precisely place ROI inside the ablated tumor. Thus, Z_{eff} obtained 1 month or later might have included the value of marginal parenchyma to a certain degree. Although this study suggests the possibility of

detecting local tumor progression with tumor composition analysis, we could not show that the Z_{eff} was truly useful for diagnosing a local progression because this study did not include any tumors with local progression. This should be addressed in a future study. Lung perfusion scintigraphy and SPECT/CT were performed only for the patients in whom lung perfusion analysis was positive for decreased perfusion. This indicates that our study may include false-negative results for decreased perfusion, based on lung perfusion analysis. Two cases of decreased perfusion on iodine map images were not confirmed by lung perfusion scintigraphy, demonstrating false-positive results on lung perfusion analysis. In actuality, the iodine map images were not always very clear. For example, emphysematous lungs showed a heterogeneous iodine map density of the parenchyma, which made the evaluation difficult. Furthermore, artifact due to pulsation of the heart and the administration of contrast material interfered with appropriate evaluation. Finally, 28% (14/50) of the tumors were excluded from analysis of tumor composition or lung perfusion, which may be a limitation of those analyses.

In conclusion, DECT was useful for evaluating RFA of lung tumors by providing additional information on tumor composition and lung perfusion.

References

1. Wisenbaugh ES, Paden RG, Silva AC, et al. Dual-energy vs conventional computed tomography in determining stone composition. Urology 2014;83:1243–1247.

2. Li M, Zheng X, Li J, et al. Dual-energy computed tomography imaging of thyroid nodule specimens: comparison with pathologic findings. Invest Radiol 2012;47:58–64.

3. Nakazawa T, Watanabe Y, Hori Y, et al. Lung perfused blood volume images with dual-energy computed tomography for chronic thromboembolic pulmonary hypertension: correlation to scintigraphy with single-photon emission computed tomography. J Comput Assist Tomogr 2011;35:590–595.

4. Thieme SF, Graute V, Nikolaou K, et al. Dual energy CT lung perfusion imaging—correlation with SPECT/CT. Eur J Radiol 2012;81:360–365.

5. Dupuy DE, Zagoria RJ, Akerley W, et al. Percutaneous radiofrequency ablation of malignancies in the lung. AJR 2000;174:57–59.

6. Hiraki T, Gobara H, Iguchi T, et al. Radiofrequency ablation for early-stage nonsmall cell lung cancer. Biomed Res Int 2014;2014:152087.

7. Hiraki T, Gobara H, Iguchi T, et al. Radiofrequency ablation as treatment for pulmonary metastasis of colorectal cancer. World J Gastroenterol 2014;20:988–996.

8. Blind for review

9. Abtin FG, Eradat J, Gutierrez AJ, et al. Radiofrequency ablation of lung tumors: imaging features of the postablation zone. Radiographics 2012;2:947–969.

10. Lee SH, Lee JM, Kim KW, et al. Dual-energy computed tomography to assess tumor response to hepatic radiofrequency ablation: potential diagnostic value of virtual noncontrast images and iodine maps. Invest Radiol 2011;46:77-84.

11. Park SY, Kim CK, Park BK. Dual-energy CT in assessing therapeutic response to radiofrequency ablation of renal cell carcinomas. Eur J Radiol 2014;83:e73-79.

12. Goodsitt MM, Christodoulou EG, Larson SC. Accuracies of the synthesized monochromatic CT numbers and effective atomic numbers obtained with a rapid kVp switching dual energy CT scanner. Med Phys 2011;38:2222–2232.

13. Steinke K, Haghighi KS, Wulf S, et al. Effect of vessel diameter on the creation of ovine lung radiofrequency lesions *in vivo*: preliminary results. J Surg Res 2005;124:85–91.

Figure legends

Figure 1. CT images of the ROI placement. Before and 2 days after RFA, the ROI was placed onto the tumor as large as possible (A, B). The ROI was placed at the center of the ablation zone 1 month (C), 3 months (D), and 6 months (E) after RFA.

Figure 2. Mean effective atomic number **(**Z_{eff}) and 95% confidence interval of the lung tumors before radiofrequency ablation (RFA) and at 2 days, 1 month, 3 months, and 6 months after RFA. There are significant differences between the Z_{eff} before RFA and the Z_{eff} at 2 days, 1 month, 3 months, and 6 months ($P < 0.001$ for each comparison).

Figure 3. 79-year-old man with a metastatic lung tumor. (A) CT image before radiofrequency ablation (RFA) shows an 8-mm diameter tumor (arrow) in the left lower lobe. (B) Iodine map image before RFA. (C) CT image 2 days after RFA shows ablation zone (arrowheads). (D) Iodine map image 2 days after RFA shows decreased perfusion of peripheral lung parenchyma (arrows) as well as ablation zone (arrowheads). (E) SPECT/CT image 2 days after RFA shows decreased perfusion of peripheral lung parenchyma (arrows) as well as ablation zone (arrowheads), which is similar to iodine map image (D).

Figure 4. 43-year-old woman with recurrent primary lung cancer. (A) CT image before radiofrequency ablation (RFA) shows a 13-mm diameter tumor (arrow) in the left lower lobe. (B) The iodine map image before RFA. (C) CT image 2 days after RFA shows ablation zone (arrowheads). (D) Iodine map image 2 days after RFA shows decreased perfusion of peripheral lung parenchyma (arrows) as well as ablation zone (arrowheads). Note that a pulmonary artery and its branch (arrows, B), which were patent before RFA, are not demonstrated after RFA. (E) SPECT/CT image 2 days after RFA shows decreased perfusion of peripheral lung parenchyma (arrows) as well as ablation zone (arrowheads), which is similar to iodine map image (D).

(#4) Figure1A

Click here to download (#4) Figure, Please list figure number in Description box (NO JPEGS) FIG1A.TIF.tif

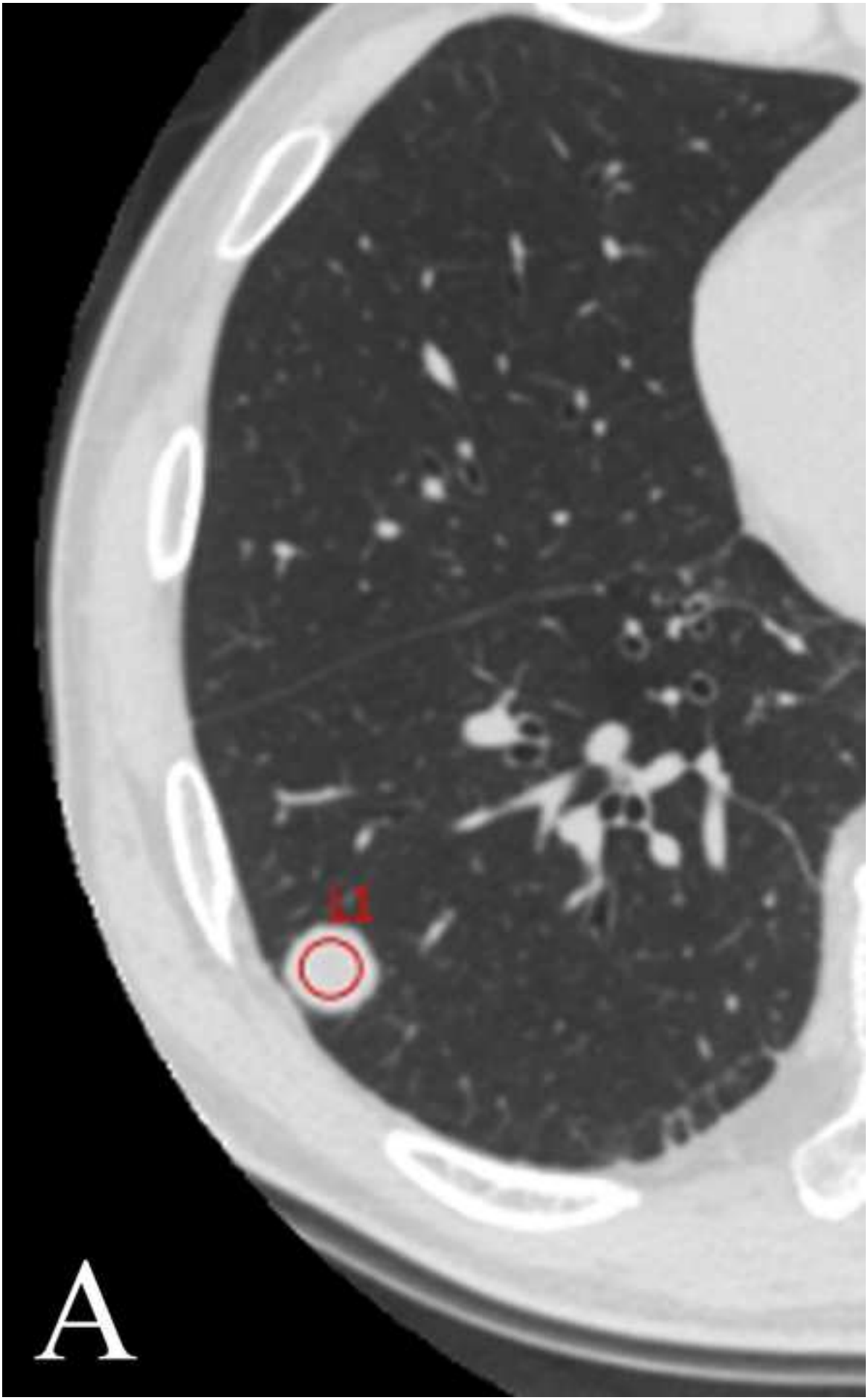

(#4) Figure1B

Click here to download (#4) Figure, Please list figure number in Description box (NO JPEGS) FIG1B.TIF.tif

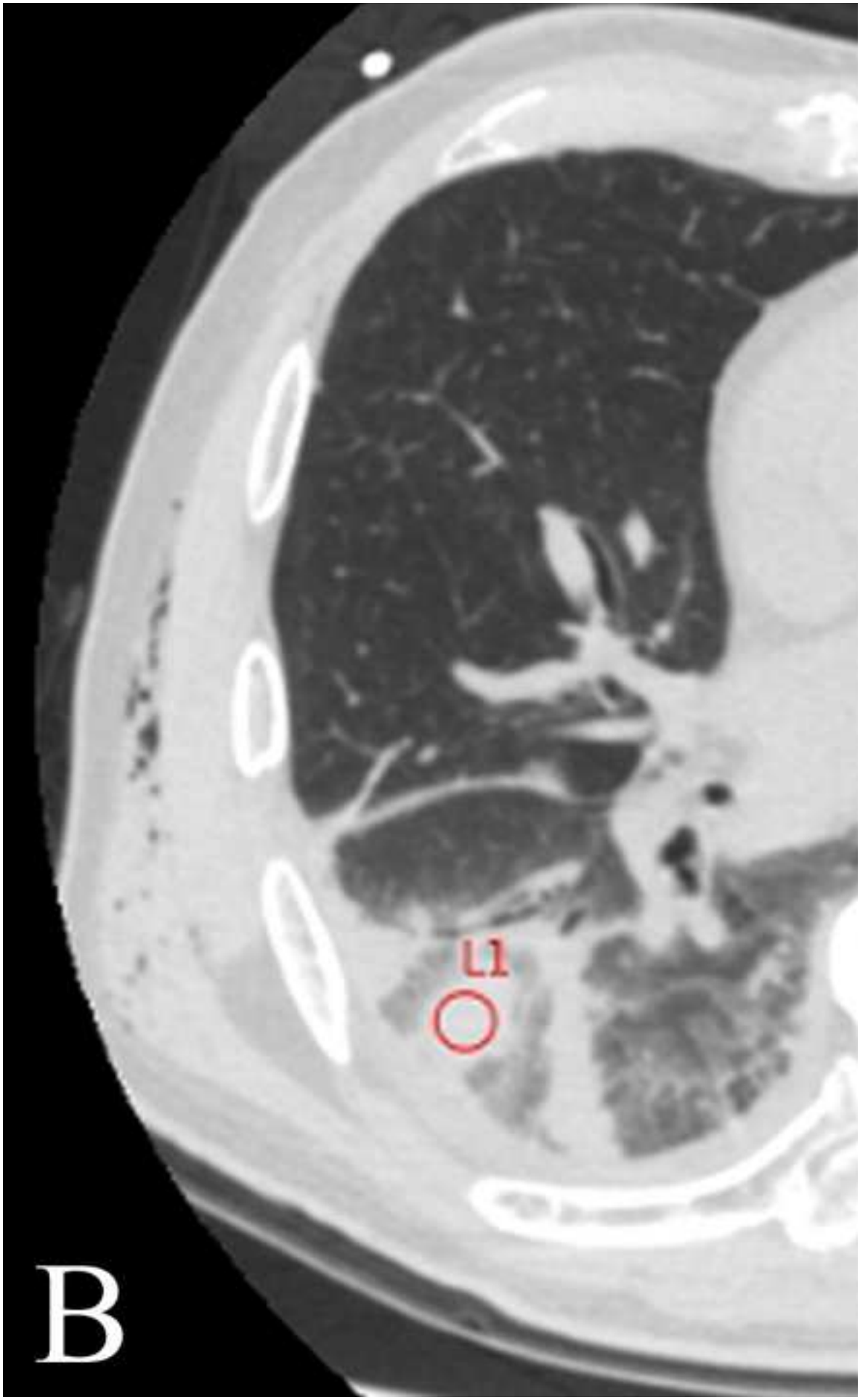

(#4) Figure1C

Click here to download (#4) Figure, Please list figure number in Description box (NO JPEGS) FIG1C.TIF.tif

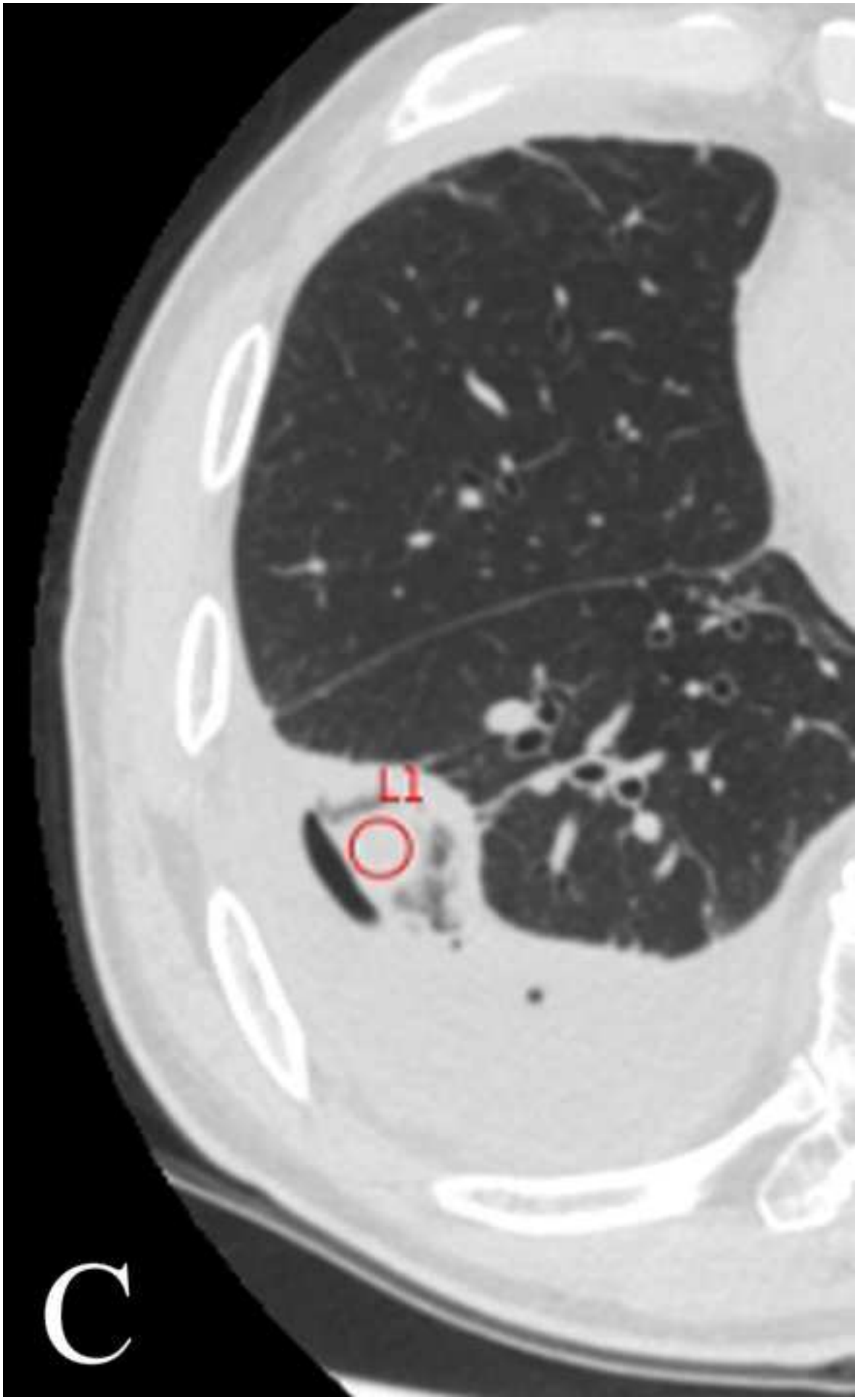

(#4) Figure1D

Click here to download (#4) Figure, Please list figure number in Description box (NO JPEGS) FIG1D.TIF.tif

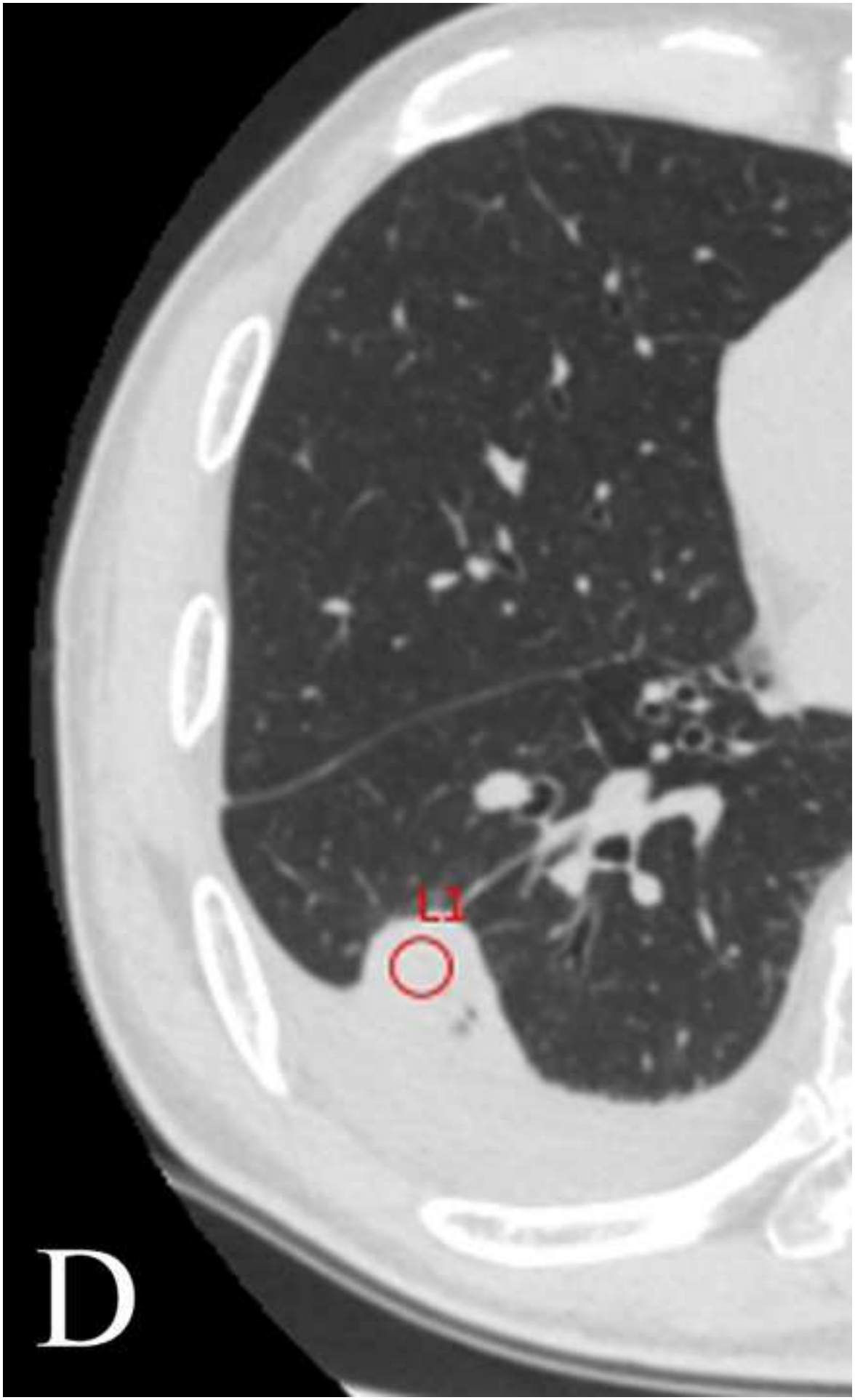

(#4) Figure1E

Click here to download (#4) Figure, Please list figure number in Description box (NO JPEGS) FIG1E.TIF.tif

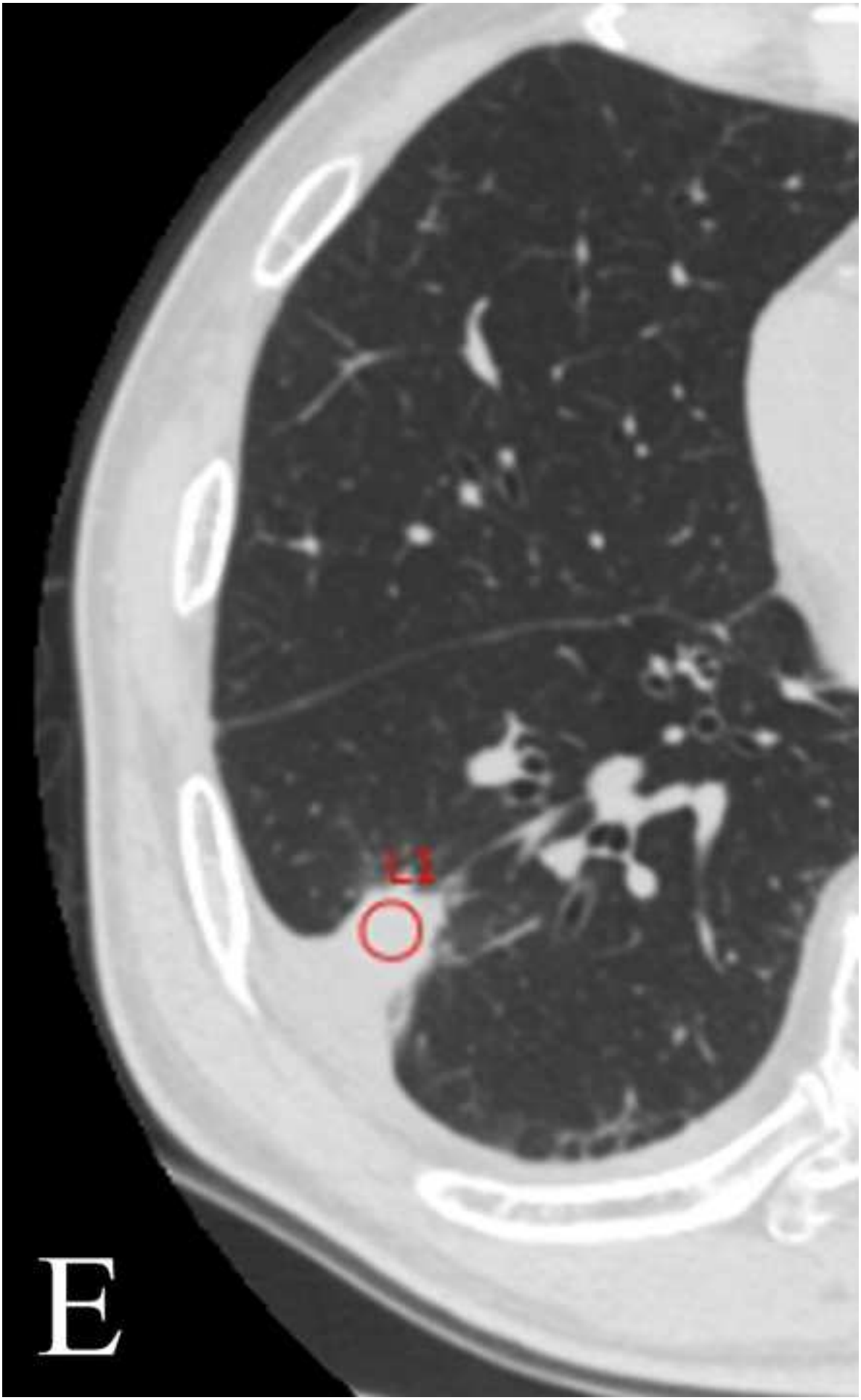

(#4) Figure2

Click here to download (#4) Figure, Please list figure number in Description box (NO JPEGS) FIG2.TIF.tif

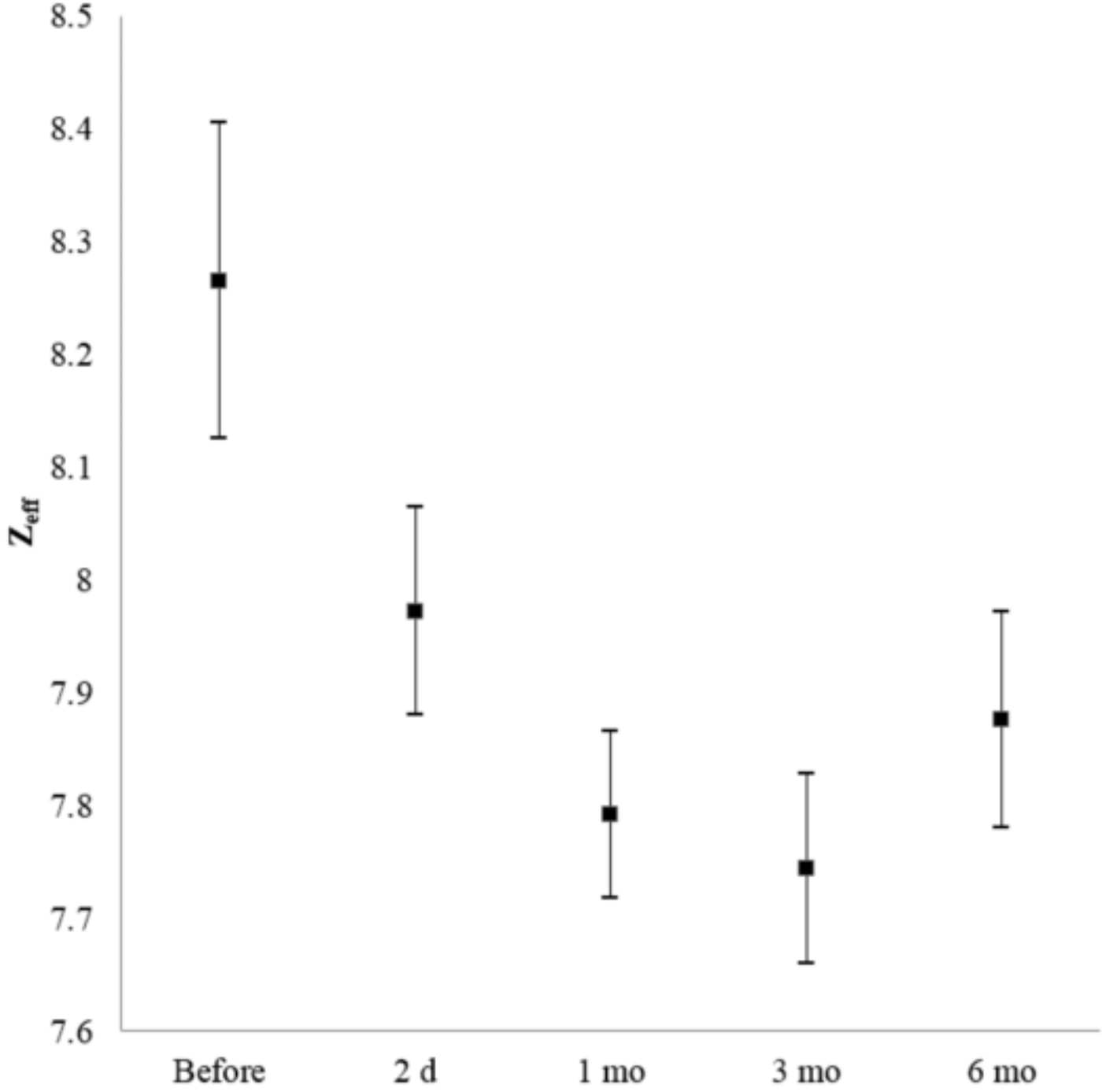

(#4) Figure3B

Click here to download (#4) Figure, Please list figure number in Description box (NO JPEGS) FIG3B.TIF.tif

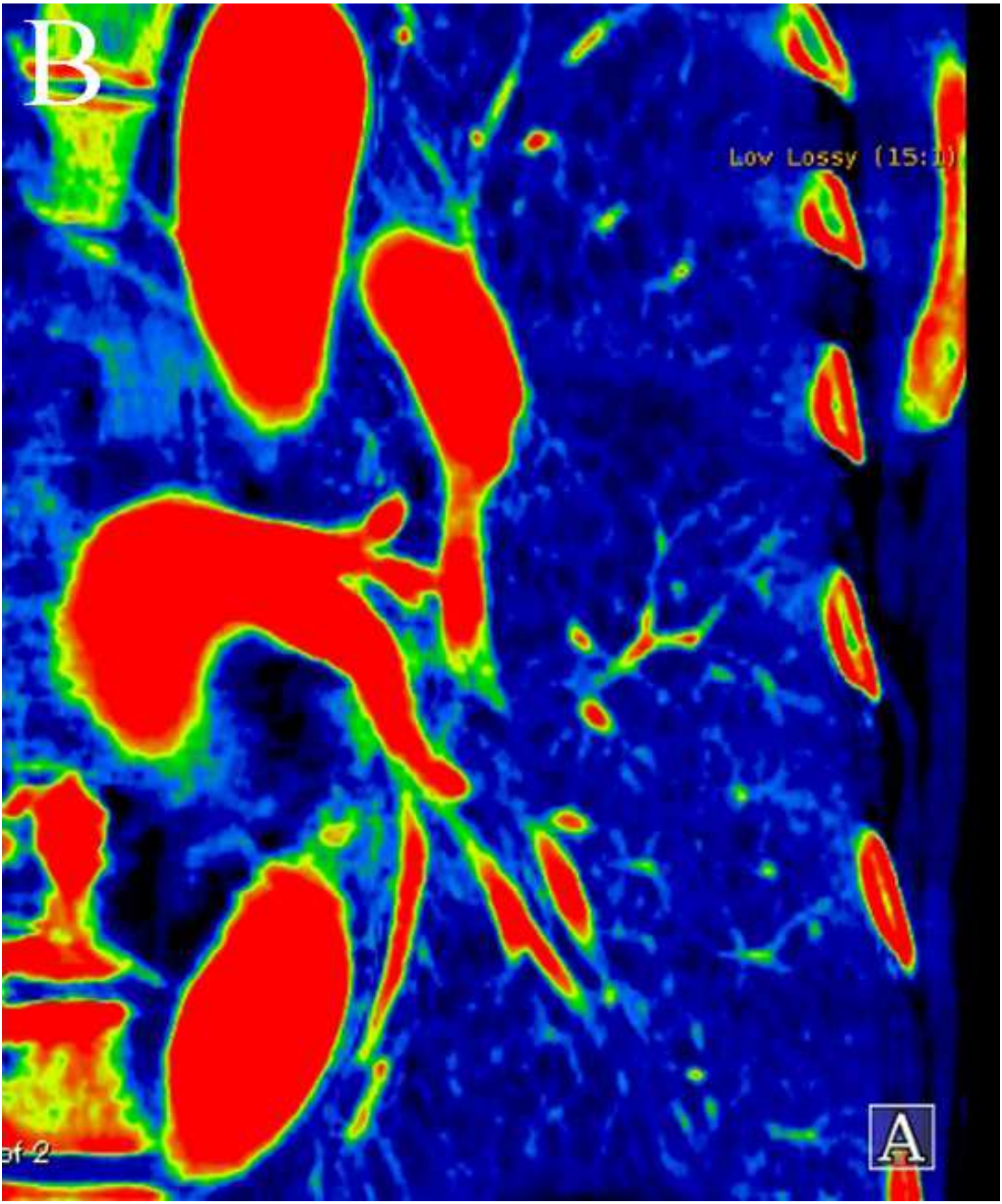

(#4) Figure3C

Click here to download (#4) Figure, Please list figure number in Description box (NO JPEGS) FIG3C.TIF.tif

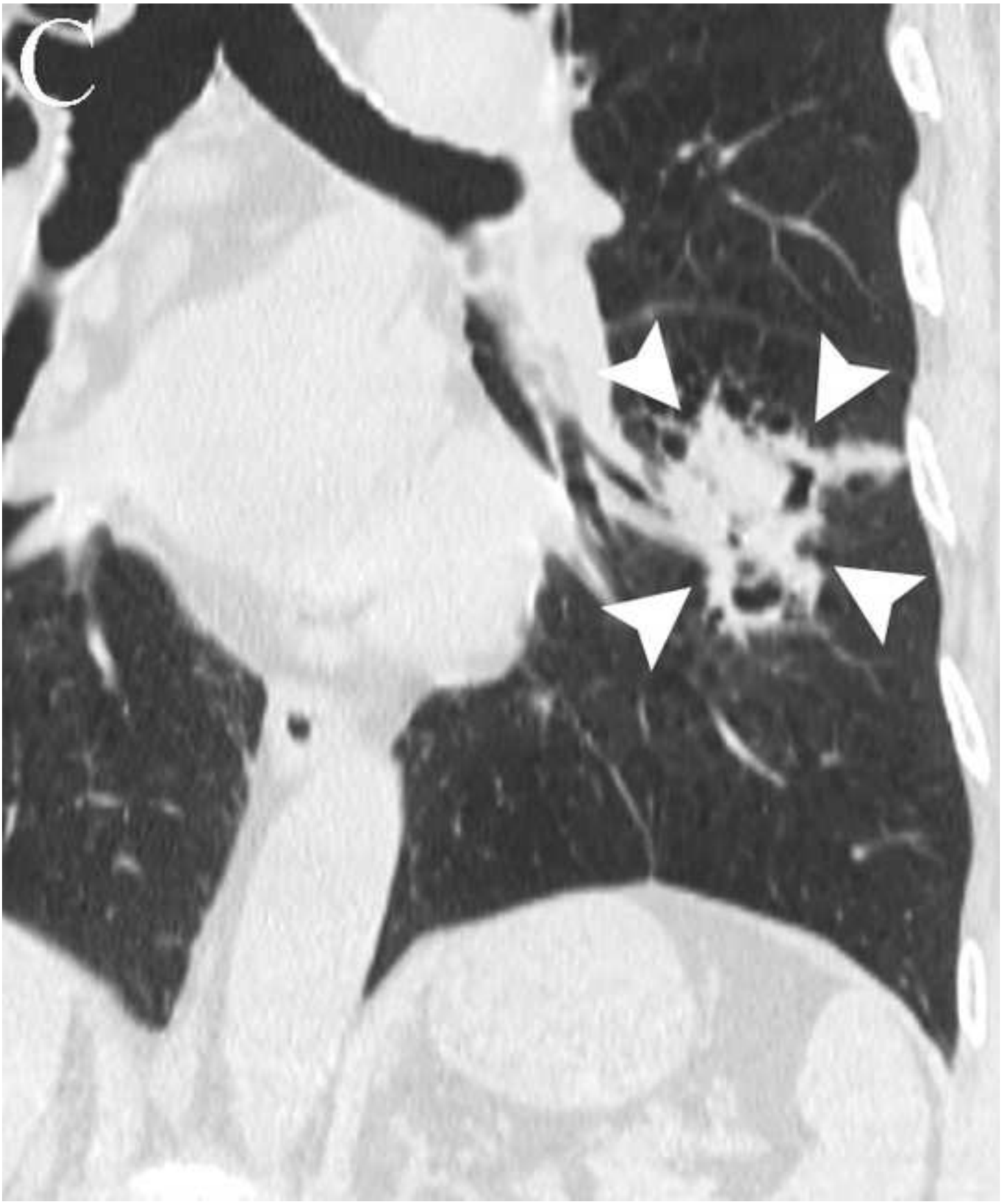

(#4) Figure3D

Click here to download (#4) Figure, Please list figure number in Description box (NO JPEGS) FIG3D.TIF.tif

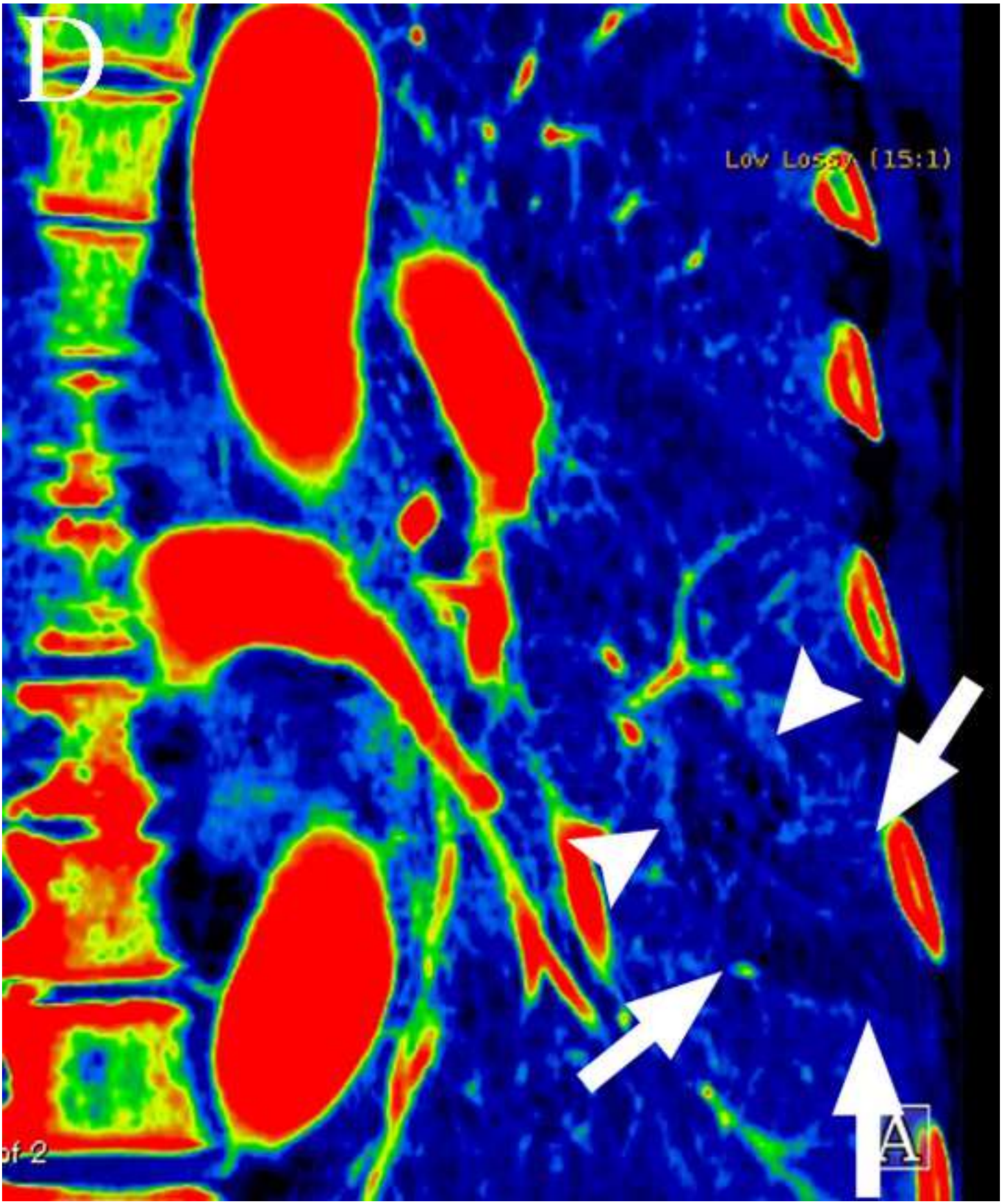

(#4) Figure3E

Click here to download (#4) Figure, Please list figure number in Description box (NO JPEGS) FIG3E.TIF.tif

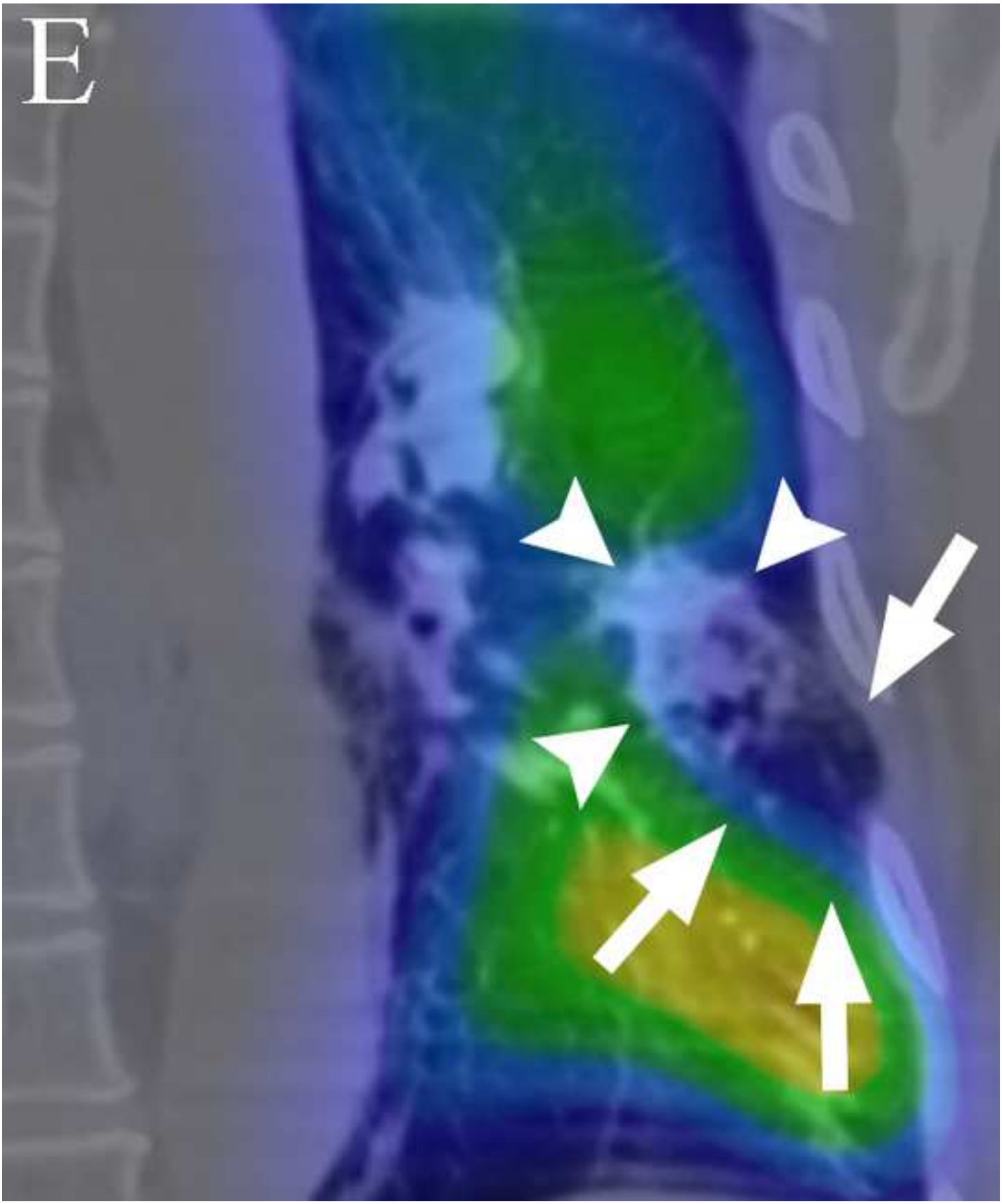

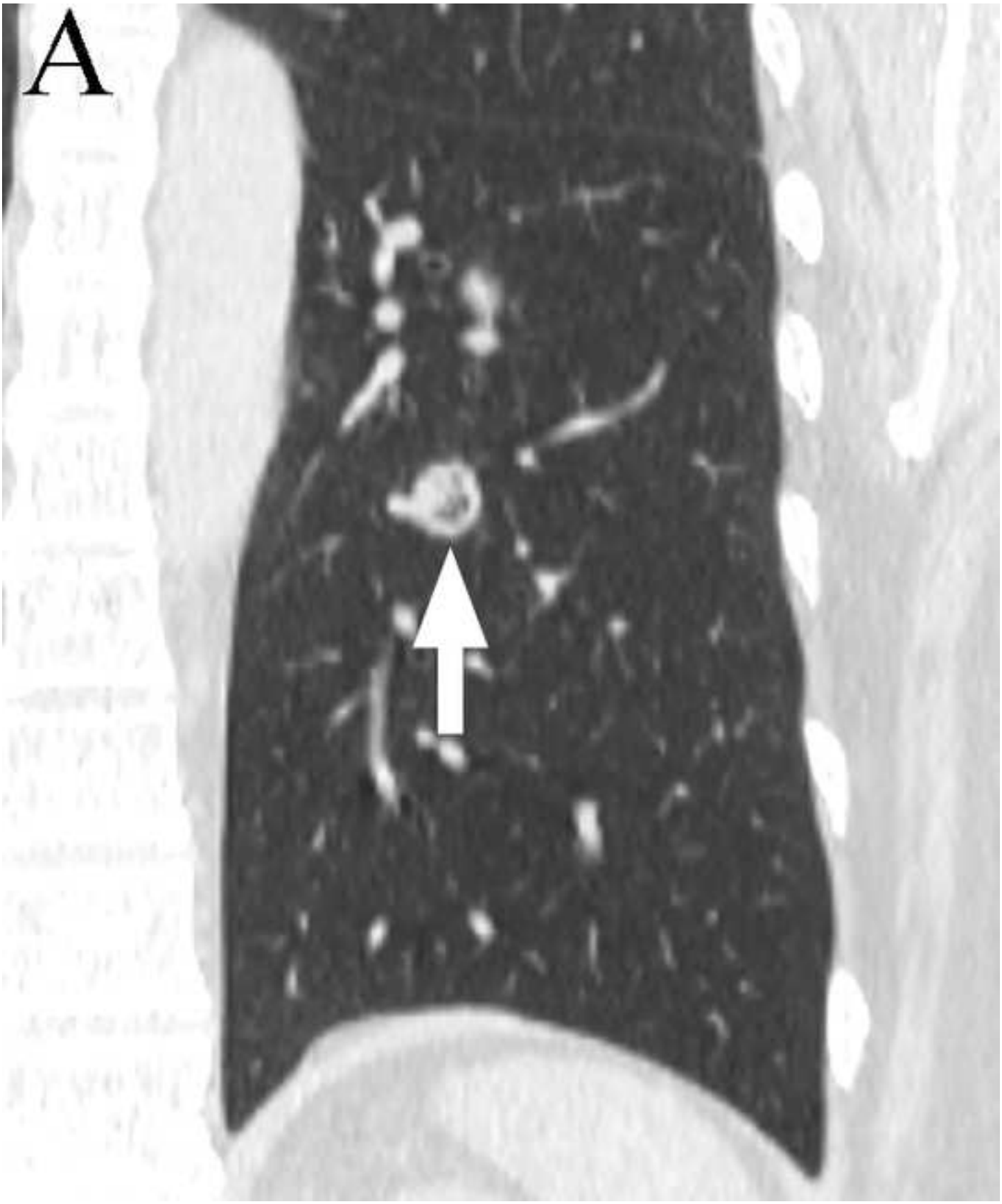

(#4) Figure4B

Click here to download (#4) Figure, Please list figure number in Description box (NO JPEGS) FIG4B.TIF.tif

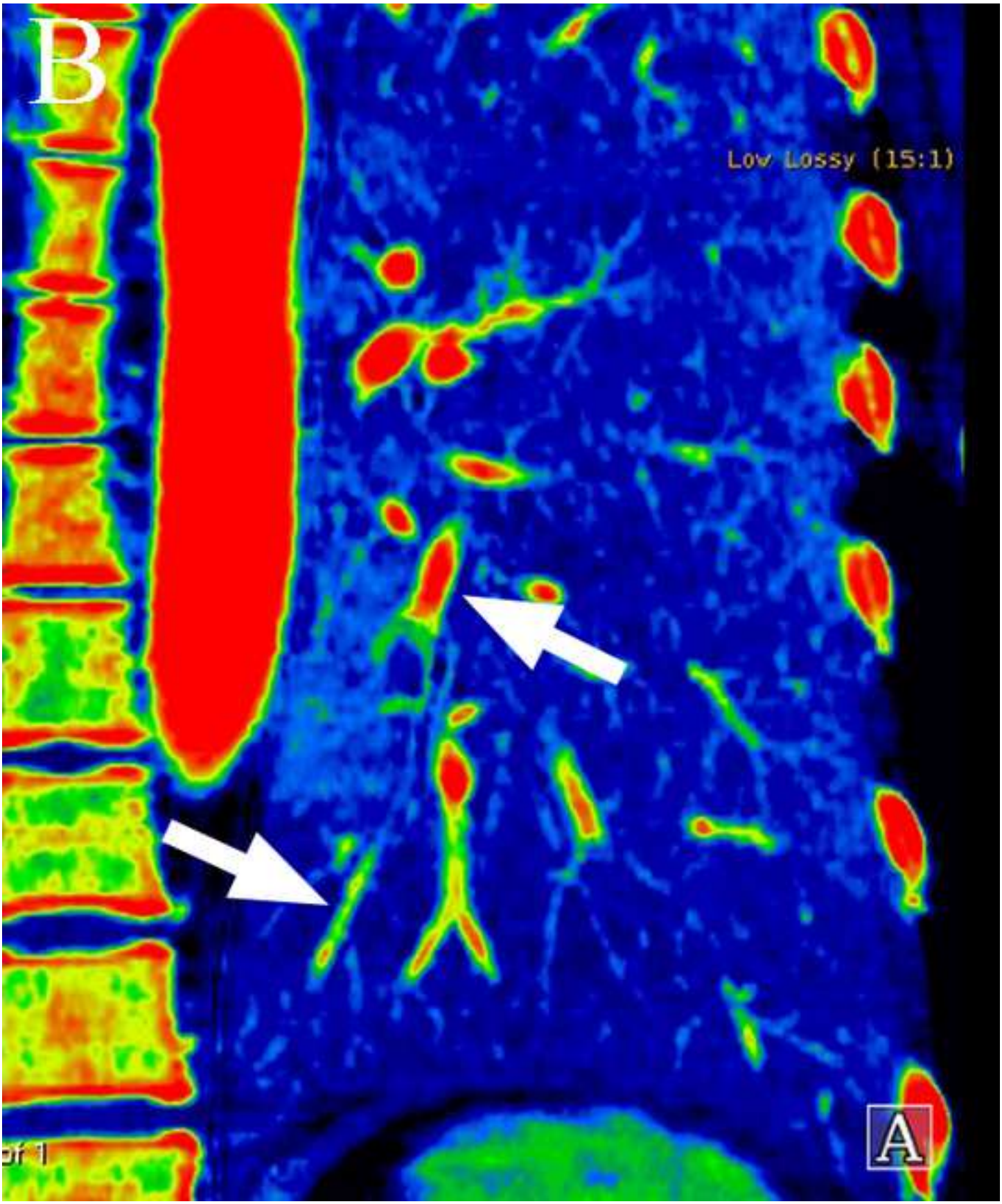

(#4) Figure4D

Click here to download (#4) Figure, Please list figure number in Description box (NO JPEGS) FIG4D.TIF.tif

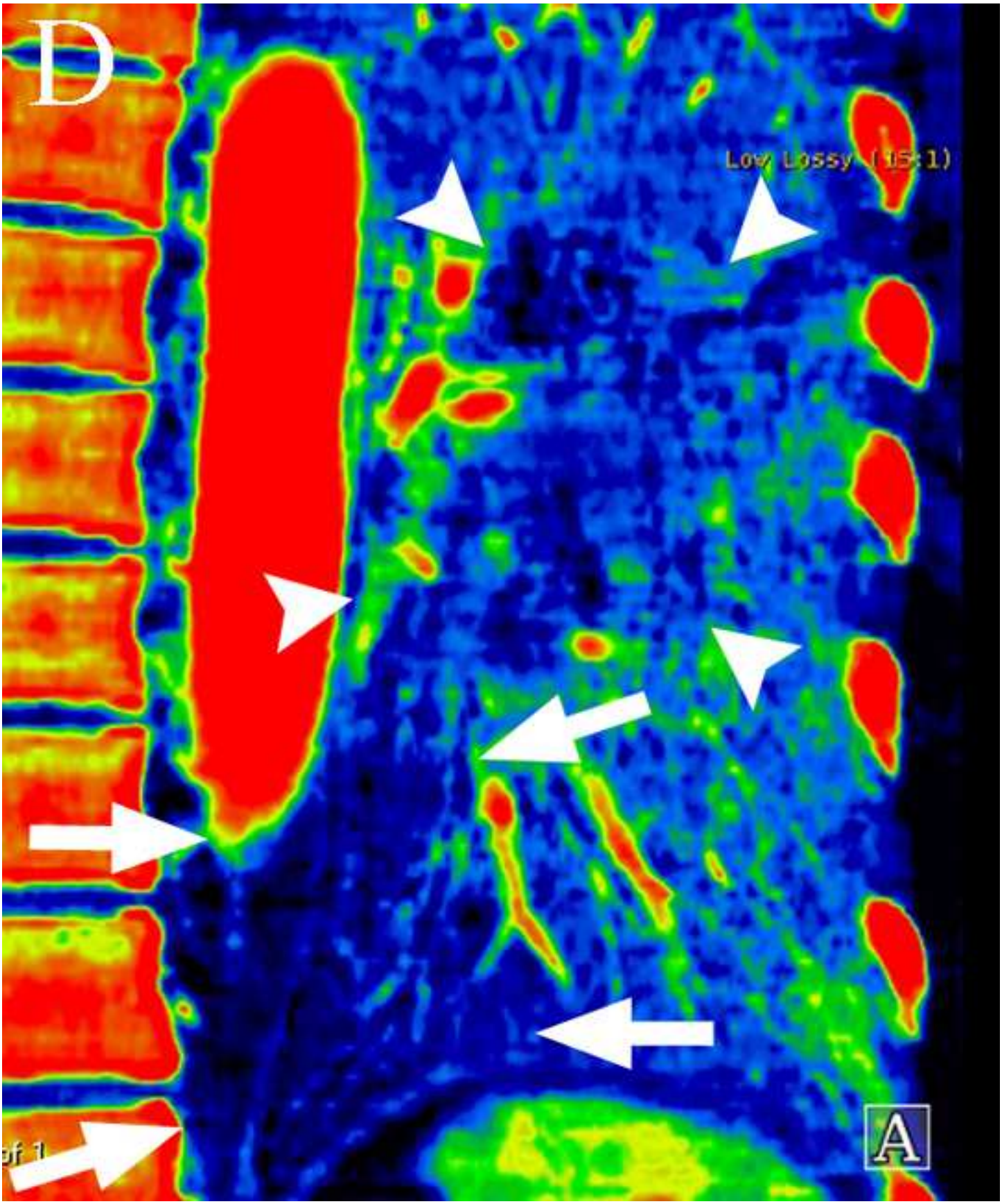

(#4) Figure4E

Click here to download (#4) Figure, Please list figure number in Description box (NO JPEGS) FIG4E.TIF.tif

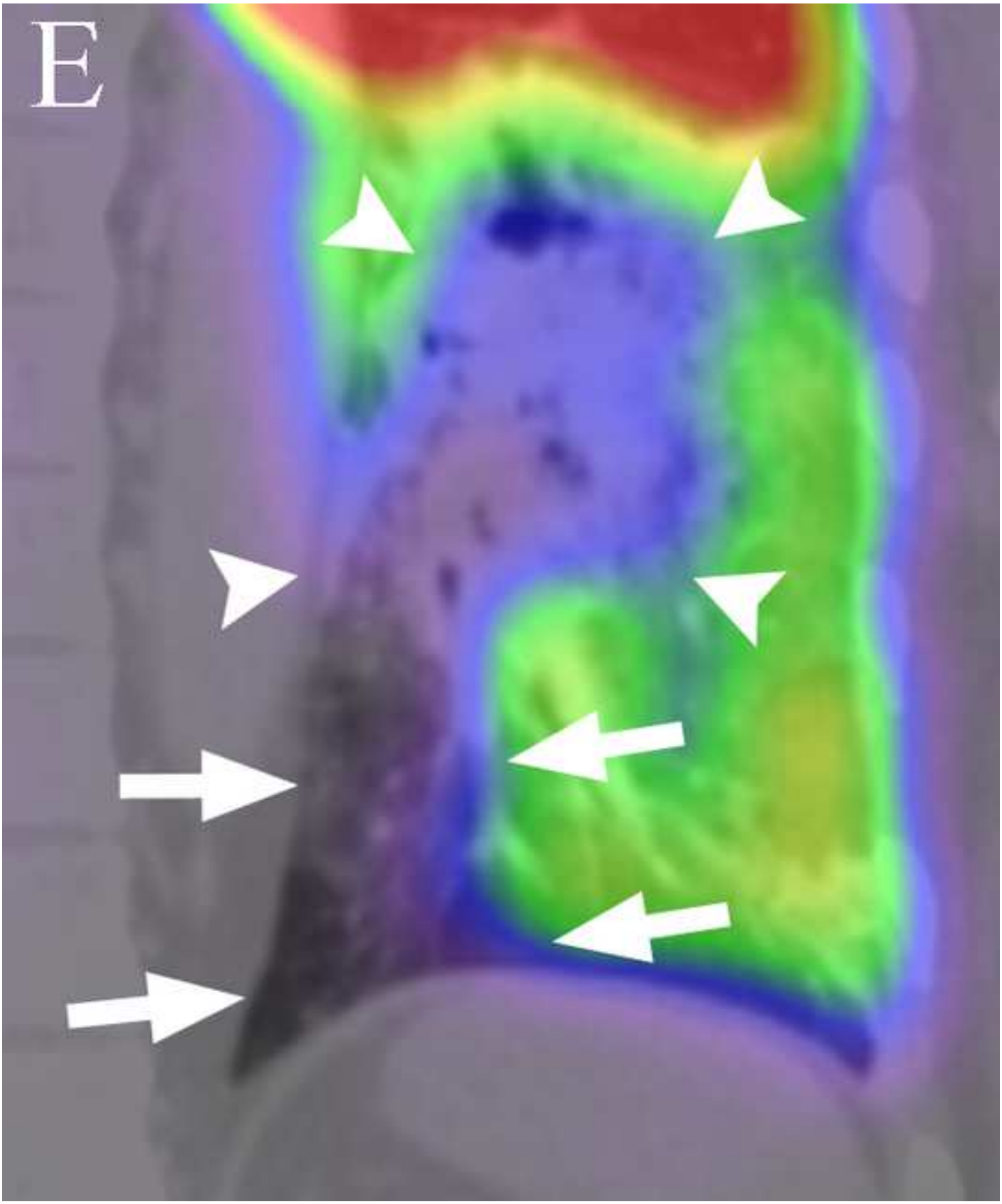

Table 1: Characteristics of the 25 Patients with 36 Tumors

Characteristic		**Value**
Age (y)	Mean（range）	61.9 (43–79)
Gender	Male	14
	Female	11
Tumor size (mm)	Mean (range)	10.00 (4–20)
Electrode	Multitined expandable	35
	Internally cooled	1
Primary lesions	Lung cancer	4
	Hypopharyngeal cancer	1
	Maxillary cancer	1
	Salivary grand cancer	2
	Gastric cancer	4
	Hepatocellular carcinoma	5

Colorectal cancer	8
Adrenal cancer	1
Renal cell carcinoma	3
Chondrosarcoma	1
Urachal cancer	1
Uterine cancer	5